Structural Engineering and Mechanics, Vol. 37, No. 6 (2011) 649-669 649
DOI: http://dx.doi.org/10.12989/sem.2011.37.6.649

Compressive behavior of short fibrous reinforced concrete members with square cross-section

G. Campione*

Dipartimento di Ingegneria Strutturale e Geotecnica, Università di Palermo, Viale delle Scienze, Palermo 90128, Italy

(Received July 28, 2009, Accepted November 23, 2010)

Abstract. In this paper an analytical model is presented that addresses the compressive response of short-fiber reinforced concrete members (FRC) with hooked steel fibers. This model is applicable to a wide range of concrete strengths and accounts for the interaction between the cover spalling and the concrete core confinement induced by transverse steel stirrups and also for buckling of longitudinal reinforcing bars. The load-shortening curves generated here analytically fit existing experimental data well.

Keywords: compression; fibers; concrete; confinement; cover spalling; buckling; load-axial strain curves; bearing capacity.

1. Introduction

Fiber reinforced concrete (FRC) is a construction material which offers important advantages with respect to plain concrete relating to its tensile resistance, especially in the post-cracking stage. Very high values of post-cracking strength and energy absorption capacity are obtained by incorporating fibers (Bentur and Mindess 1990). If poor compaction of composite is avoided by ensuring that the sand/gravel ratio in the mix design is appropriate to maintain workability with fibers, no strength reduction is observed. In this case with reference to compressive behavior, it has been shown that the addition of fibers produces significant increases in maximum and post-cracking strain values (Fanella and Naaman 1983, Nataraja *et al*. 1999, Campione *et al*. 1999). Other positive effects of using fibers were observed in compressed members after the peak load was reached and primarily an increase in apparent ductility, as shown in Foster (2001) and in Campione (2002).

Recent studies (e.g., Fosters 2001, Saeker 2001, Campione 2002, Zaina and Foster 2005, Bencardino *et al*. 2008, Aoude *et al*. 2009) have shown that for structural applications relating to reinforced concrete columns, fibers can be successfully used in combination with traditional steel reinforcements, allowing a reduction in the required percentages of transverse steel reinforcement, especially in seismic design. In this case the presence of fibers can mitigate or prevent longitudinal bar buckling (Dhakal 2006), thereby reducing the cover spalling process and also increasing the effectively confined core.

*Corresponding author, Associate Professor, E-mail: campione@stru.diseg.unipa.it

In the present paper the focus is on the advantages of using hooked steel fibers in conventionally reinforced members in compression. Specifically, the paper stresses the influence of fibers on the spalling process of the concrete cover and on the overall stability of longitudinal bars. However, no size effects are considered in this study. The original contribution is to propose a single model that considers the interaction between longitudinal bars, transverse reinforcement and confined concrete.

2. Aim and originality of the research

Research has identified two main aspects in the use of fiber reinforced concrete for columns: controlling the concrete cover spalling and reducing the critical length of the longitudinal bars. These two aspects are of fundamental importance in the design of ductile members, because a buckling length of longitudinal bars inside an R.C. member equal to or higher than the lateral spacing of stirrups can drastically reduce the confinement effects, while a premature cover spalling process, especially in high performance materials, such as high strength concretes, determines negative effects, also in terms of bearing capacity. Using FRC is of particular interest if we refer to R.C. members subjected to monotonic and cyclic axial forces and bending moment for which, as is well known, the cover spalling and buckling phenomena of compressed steel bars can drastically reduce the strength and available ductility of the member, so the use of fibers can be very suitable.

3. Analytical model for confined FRC members

The case examined is shown in Fig. 1 and refers to a short member having a square cross-section with side b and reinforced with longitudinal steel bars with area A_{l1}, at the corners and A_{l2} along the flat portion and confined by transverse closed steel stirrups with area ϖ_{st1}, ϖ_{st2} (see Fig. 1). The stirrups are placed in the plane of the cross-section with a cover δ and they are spaced at clear spacing s. The cases examined are those shown in Figs. 1(a), 1(b) and 1(c) referring to different arrangements of longitudinal and transverse steel bars.

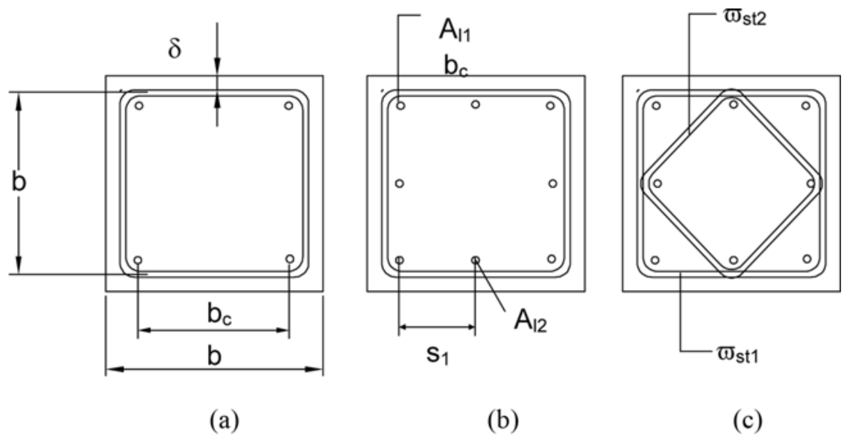

Fig. 1 Cases of steel arrangements examined with bars at the corners and single stirrup (a) no addition, (b) four additional bars, (c) four additional bars and double stirrup

If loaded in compression, columns exhibit shortening accompanied by lateral deformation inducing stresses in concrete and in steel proportional to their axial stiffness. The concrete cover close to the transverse stirrups behaves as a compressed shell having low thickness (δ) and essentially subjected to a biaxial state of stresses (compression-tension). The concrete core is subjected to a triaxial state of stresses (compression-compression), while the main bars are in compression.

In the following sections preliminarily to the determination of the load-axial strain curves of columns, the stress-strain curves of constituent materials (concrete cover, core and steel bars) will be introduced and validated on the basis of existing experimental data. Then a comparison will be made between the complete compressive response of short reinforced fibrous concrete columns with experimental tests available in the literature.

4. Stress-strain curves for unconfined and confined FRC

It has been widely observed experimentally that the addition of hooked short steel fibers in plain concrete significantly affects the post-peak response of plain concrete, especially referring to the ductility resources underlined by higher strain capacity and reduced slope of the softening branch of the response (see e.g., Foster 2001, Bencardino *et al*. 2008, Aoude *et al*. 2009). These effects also depend on concrete strength and type (normal or lightweight) (see e.g., Campione and La Mendola 2001).

4.1 Stress-strain in compression for unconfined concrete

For unconfined plain concrete, the following stress-strain relationship (Sargin 1971) is adopted in this work

$$\sigma = f_c \cdot \frac{\left(\frac{\varepsilon}{\varepsilon_0}\right) \cdot \beta}{\beta - 1 + \left(\frac{\varepsilon}{\varepsilon_0}\right)^{\beta}} \tag{1}$$

β is a parameter which modulates the slope of the softening branch of the response and take on the value

$$\beta = \frac{E_c}{E_c - \frac{f_c}{\varepsilon_0}} \tag{2}$$

where E_c is the initial elasticity tangent modulus, and f_c and ε_0 the peak stress and the corresponding strain values.

In the absence of experimental data, E_c can be assumed, as suggested in Razvi and Saatcioglu (1999) for different concrete strengths, in the form $E_c = 6900 + 3320 \cdot \sqrt{f_c}$ (in MPa).

Eq. (1), originally assumed for normal strength concrete, covers a wide range of experimental data referring to several concrete grades if the peak strain ε_0 and the β parameter are assumed to be variable with the peak strength according to the following equations with f_c expressed in MPa

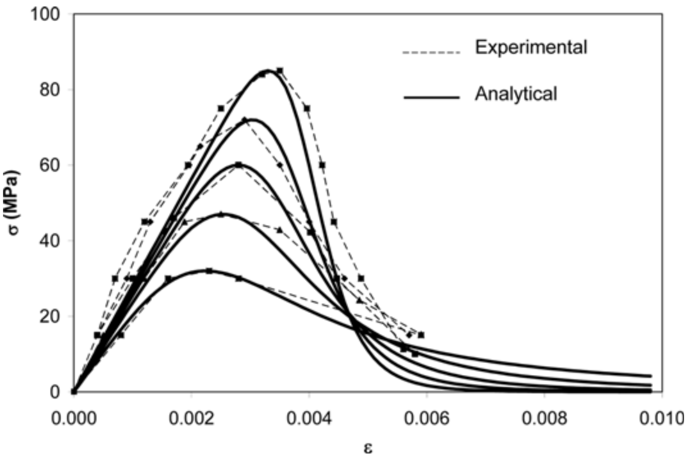

Fig. 2 Stress-strain curve for unconfined concrete (data of Ahmad and Shah 1985)

$$\varepsilon_0 = 0.0016 + 0.00002 \cdot f_c \tag{3}$$

$$\beta = 1.4276 \cdot e^{(0.0247 \cdot f_c)} \tag{4}$$

Eq. (3) and Eq. (4) are here derived in such a way as to give the best fitting with the experimental curves given by Ahmad and Shah (1985) referring to several concrete grades.

Fig. 2 shows the stress-strain curves from Eq. (1), where ε_0 and β are defined in Eqs. (3) and (4), and the experimental curves given by Ahmad and Shah (1985).

In the case of fibrous concrete it was observed experimentally (see e.g., Campione *et al*. 1999, Fanella and Naaman 1985, Hsu and Hsu 1994) that for hooked steel fibers, if good compaction of concrete is ensured, the peak stress f_{cf}, the corresponding strain ε_{cf} and the slope of the softening branches change. These benefits increase with an increase in the reinforcing index F defined as $F = v_f \cdot L_f / \phi_f$. v_f, L_f and ϕ_f are respectively the volume percentage, length and diameter of the hooked end fibers

On the basis of Campione (2007) Eq. (1) can also be adopted for FRC with steel fibers and these parameters can be related to F through the following relationships

$$f_{cf} = f_c + 6.913 \cdot F \text{ (in MPa)} \tag{5}$$

$$\varepsilon_{0f} = \varepsilon_0 + 0.00192 \cdot F \tag{6}$$

$$\beta_1 = \beta + 0.175 \cdot F \tag{7}$$

Using Eq. (1), β is replaced with β_1 for $\varepsilon > \varepsilon_{of}$ while Eq. (4) is assumed for $\varepsilon < \varepsilon_{of}$.

Fig. 3 shows a comparison between the stress-strain curves in compression obtained with the proposed model (Eq. (1) by means of Eqs. (5), (6), (7)) and some experimental ones given in the literature for normal and high strength fibrous concrete with hooked steel fibers with $L_f/\phi_f = 60$. Specifically, the experimental data of Fanella and Naaman (1985) refer to compressive tests on 100×200 mm normal strength plain and FRC concrete cylinders with hooked steel fibers at volume percentages of 0.7 and 1.4%; while the experimental data generated by Hsu and Hsu (1994) refer to

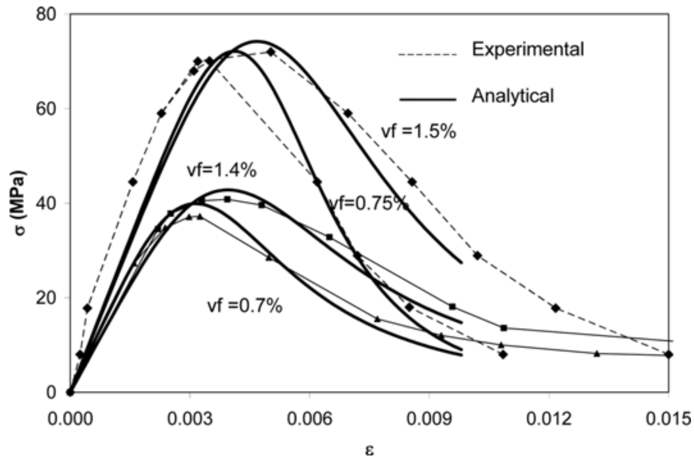

Fig. 3 Experimental and analytical stress-strain curve for FRC with hooked steel fibers: NSC data of Fanella and Naaman (1985), HSC of HSU and Hsu (1994)

compressive tests on 100 × 200 mm high strength plain and FRC concrete cylinders with hooked steel fibers at volume percentages of 0.75 and 1.5%. In both cases examined a comparison shows the capacity of the proposed analytical equation to fit the experimental results.

With reference to compressive behavior the compressive peak stress and corresponding strain were reduced considering the softening coefficient proposed in the literature by Michell *et al.* (1986) in the form

$$\varsigma = \frac{5.8}{\sqrt{f_c'}} \frac{1}{\sqrt{1+400 \cdot \varepsilon_t}} \le \frac{0.9}{1+400 \cdot \varepsilon_t} \tag{8}$$

With ε_t the lateral strain is related to the axial strain ε through the Poisson coefficient ν_c ($\varepsilon_t = \nu_c \varepsilon$). The Poisson coefficient can be assumed to vary with the axial strain ε, as suggested in Elwi and Murray (1979), with the expression

$$\nu = \nu_0 \cdot \left[1 + 1.38 \cdot \frac{\varepsilon}{\varepsilon_{cu}} - 5.36 \cdot \left(\frac{\varepsilon}{\varepsilon_{cu}}\right)^2 + 8.59 \cdot \left(\frac{\varepsilon}{\varepsilon_{cu}}\right)^3\right] \tag{9}$$

In Eq. (9) ε_{cu} is the ultimate strain in the concrete cover (the complete cover is spalled off), and it is assumed to be 0.004 (e.g., as suggested in Mander *et al.* 1988).

The softening coefficient ς affecting f_c' and ε_0 takes into account the biaxial state of stresses (compression-tension) induced in the concrete cover by the compressive load.

As observed by Demeke and Tegos (1994) the inclusion of steel fibers in concrete members substantially improves their biaxial strength. Fiber reinforced concrete strength under combined tension and compression is far greater than plain concrete strength and steel fibers increase concrete strength from one to three times depending of the amount of fiber.

According to ACI 318 (2002) the range of variation of the efficiency factor is between 0.4 and 1 depending on the strut geometry. Values in the ranger from 0.4-0.8 are obtained for plain concrete by using Eq. (8), assuming $\nu = 0.5$ and $\varepsilon_{cu} = 0.004$.

In the case of FRC a linear variation in the softening coefficient with F can be assumed, as already done in Campione *et al.* (2009). In this case the efficiency factor ξ_{FRC} for FRC is related to that of plain concrete in the form $\xi_{FRC} = \xi + 0.28 \cdot F$. This assumption is in agreement with experimental results obtained by Demeke and Tegos (1994).

4.2 Stress-strain curves in compression for confined concrete

Several models are available in the literature for analyzing the confinement effects produced by transverse steel reinforcements on compressed normal and high strength concrete (NSC, HSC) members with circular, square or rectangular cross-section reinforced with longitudinal and transverse bars (see e.g., Cusson and Paultre 1995, Razvi and Saaatcioglu 1999). More recently some other models have become available for confined fibrous reinforced concrete (see e.g., Foster 2001, Campione 2002). These models allow one to evaluate the strength and strain enhancements due to transverse steel and give the stress-strain curves in compression, also including the post-peak response.

Referring to the maximum compressive strength f_{cc} of ordinary confined concrete members Cusson and Paultre (1995) showed that the relationship between f_{cc} and the effective confinement pressure f_{le} is nonlinear and can be expressed in the form

$$\frac{f_{cc}}{f_c} = 1 + 2.1 \cdot \left(\frac{f_{le}}{f_c}\right)^{0.7} \tag{10}$$

As suggested in Campione (2002) for FRC compressed members it is possible to use Eq. (10) by computing the effective confinement pressure with the procedure proposed by Mander *et al*. (1988), but taking the presence of fibers into account. The effect of the latter, as suggested in Campione (2002), is reflected in higher confinement pressures due to the presence of the concrete cover and in a bigger effectively confined core.

For the calculation of the confinement pressure at hoop level the equilibrium condition of half a cross-section considered as a rigid body (see Fig. 4) was applied, the confinement pressure proving to have the following form

$$f_l = \left(\frac{2 \cdot \omega_{stl}}{b_c \cdot s} + \sqrt{2} \cdot \frac{\omega_{st2}}{b_c \cdot s}\right) \cdot \sigma_s(\varepsilon_t) + f_t(\varepsilon_t) \cdot \frac{2 \cdot \delta \cdot s}{b_c \cdot s} \tag{11}$$

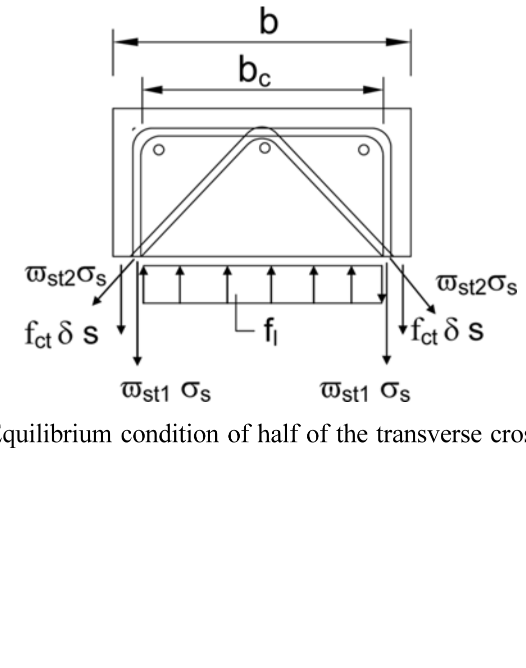

Fig. 4 Equilibrium condition of half of the transverse cross-section

If stirrups have yielded at stress f_y and therefore the post-cracking strength f_r has been attained in the composite, the maximum confinement pressure proves to be

$$f_{l\max} = \left(\frac{2 \cdot \omega_{st1}}{b_c \cdot s} + \sqrt{2} \cdot \frac{\omega_{st2}}{b_c \cdot s}\right) \cdot f_y + \frac{2 \cdot \delta}{b_c} \cdot f_r \tag{12}$$

Referring to the post-cracking strength of FRC in tension, it was shown that it is possible to relate its value to the strength characteristics of plain concrete and to the geometrical and mechanical characteristics of fibers. Specifically, it was shown that the maximum tensile strength can be assumed to be that of plain concrete, while the post-cracking tensile strength can be assumed, as suggested in Campione *et al*. (2006), to be

$$f_r = 0.2 \cdot F \cdot (f_{cf})^{0.5} \quad \text{in MPa} \tag{13}$$

The effectively confined core was referred to the Mander *et al*. (1988) model, which with reference to the cases in Fig. 2 gives the following expressions for the k_e coefficients

$$k_e = \frac{\left(1 - \sum_{i=1}^{4} \frac{(w_i)^2}{6 \cdot b_c^2}\right) \cdot \left(1 - \frac{s_1'}{2 \cdot b_c}\right)^2}{1 - \rho_{cc}} \tag{14}$$

where ρ_{cc} is the ratio between the area of longitudinal steel reinforcements A_l and the gross area of the section Ag.

For FRC too the model of Mander *et al*. (1988) can be utilized by introducing, instead of the s' parameter (which is the clear spacing between two stirrups appearing in the expressions of the k_e factors suggested by Mander *et al*. 1988), the fictitious geometrical parameter s_1' defined in Campione (2002) as

$$s_1' = s' - 10 \cdot F \tag{15}$$

This parameter takes into account the fact that with an increase in the reinforcing index, F, the effective confined concrete core increases. Eq. (15) was obtained assuming a linear variation in s_1' with s' and F. Therefore, the effective confinement pressures can be expressed as

$$f_{le} = k_e \cdot f_l \tag{16}$$

Finally, the strain corresponding to the peak stress, as suggested in Cusson and Paultre (1995), can be assumed to be

$$\frac{\varepsilon_{cc}}{\varepsilon_0} = 1 + 5 \cdot k_1 \cdot \left(\frac{k_e \cdot f_l}{f_c'}\right)^{0.7} \tag{17}$$

with k_1 a coefficient assumed as in Cusson and Paultre (1995).

In order to determine the confined core response in terms of the stress-strain ($\sigma - \varepsilon$) curve, Eq. (1) can be adopted by replacing f_c and ε_0 with f_{cc} and ε_{cc} and calculating β though Eq. (2) referring to f_{cc} and ε_{cc}.

5. Critical length for longitudinal bars

Results for compressed normal and high strength concrete specimens in the presence of longitudinal and transverse steel bars have shown that after the cover is spalled off the risk of longitudinal bar buckling increases. If this occurs, the bars can buckle in a length L, involving several pitches, *s*, of the stirrups (see Fig. 5), leading to a dangerous reduction in the strength contribution of the main bars, which have generally yielded at this stage of loading. The assumption generally made that the buckling length is equal to the spacing of lateral stirrups is only verified when the spacing between lateral stirrups is very large and the longitudinal bars are very slender. The determination of the critical load, of the length involved, and of the forces in the stirrups is a very important problem for correct evaluation of confinement pressure. In the discrete model proposed by Papia *et al*. (1988), the compressed bars were considered connected at each pitch, *s*, to elastic-plastic springs simulating the presence of transverse steel stirrups. It was supposed that buckling, if any, can only occur in the opposite direction to the concrete core and also in the diagonal direction of the square cross-section. More recently in the discrete model proposed by Dhakal and Maekawa (2002) reinforcement stability was taken into account, also including fracture of the concrete cover in reinforced concrete members. Further study (see e.g., Dhakal 2006) based on a discrete model focused on the importance of including the effect of fibers to reduce the risk of buckling of main bars and to significantly increase the lateral strain corresponding to cover spalling.

The discrete model proposed by Papia *et al*. (1988) was modified in Russo and Terenzani (2001) by considering the axial stiffness of stirrups spread along the specimens' height. This made it possible to analyze the problem by means of an elastic beam on an elastic medium, which was represented by the spread springs simulating the stirrups subjected to tensile forces. Consequently, the evaluation of the critical load is less accurate compared to that provided by the discrete model, but a more simple solution is obtained. The approximate procedure allows one to obtain a solution which differs from the exact solution in the range of a few percent, as seen from the most common cases given in the literature.

In the present paper the continuum model was modified by introducing the contribution of the concrete cover (Foster 2001) in order to determinate the critical length.

In particular, with reference to the case shown in Fig. 6, of a square cross-section reinforced with

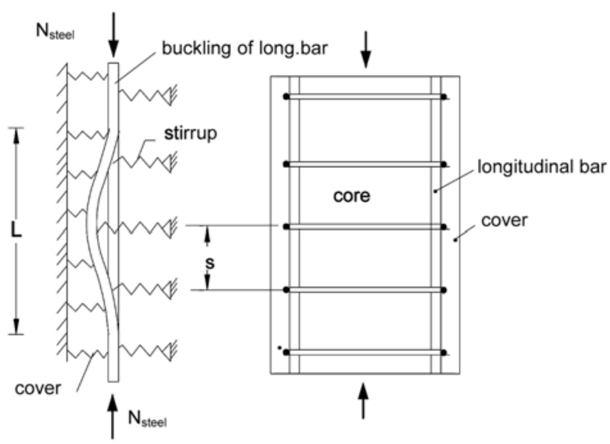

Fig. 5 Mechanical model for buckling of longitudinal bars

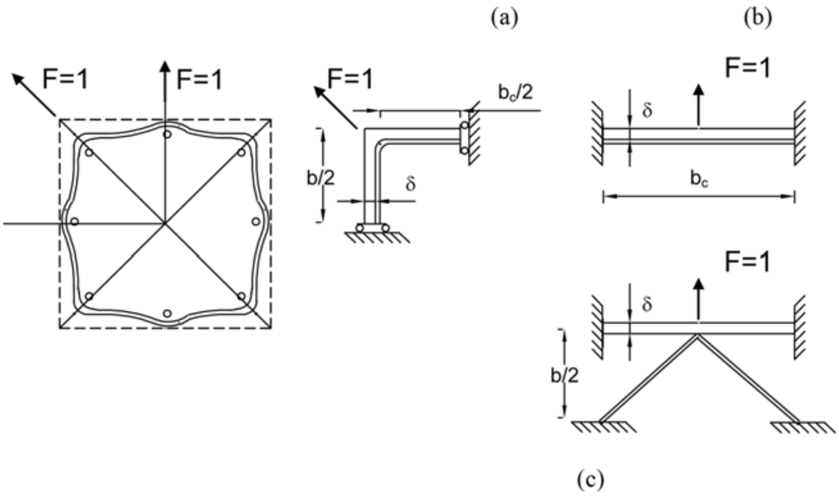

Fig. 6 Mechanical model for the calculation of equivalent spring stiffness

single closed stirrups at pitch s, and longitudinal bars at the four corners and four bars along the flat portion, it is possible to obtain the stiffness of the stirrups measured along the diagonal and along the direction perpendicular to the leg of the stirrup. This stiffness represents the force necessary to produce a unit displacement of the loaded joints.

With reference to the bar placed at the corner (see Fig. 6(a)) the stiffness of the stirrup (E_s is the elastic modulus of steel before yielding and in the plastic range is the reduced modulus here assumed to be 0.03 E_S) proves to take the form

$$\alpha_{st} = \frac{2 \cdot E_s \cdot \omega_{st1}}{b_c} \tag{18}$$

If the contribution due to the presence of the concrete cover is considered and the cover is treated, analogously to the stirrup, as a beam in tension of length $b/2$ and rectangular cross-section of sides δ and s, the equivalent spring stiffness proves to be

$$\alpha_{cover} = 2 \cdot E_{sec} \cdot \frac{\delta \cdot s}{b} \tag{19}$$

E_{sec} being the secant modulus of FRC in tension, variable for each load level and obtained by

$$E_{sec} = \frac{f_r}{\nu \cdot \varepsilon} \tag{20}$$

If the concrete cover is cracked, the post-cracking strength f_r is available for the composite, and the stiffness of the equivalent springs is reduced according to the variation in E_{sec}.

Moreover, if we refer to the case of transverse steel at first yielding and the concrete cover is cracked (in this case post-cracking strength is attained) the stiffness of the equivalent spring α_{eq} proves to be

$$\alpha_{eq} = 2 \cdot E_{sec} \cdot \frac{\delta \cdot s}{b} + \frac{2 \cdot E_s \cdot \omega_{st}}{b_c} \tag{21}$$

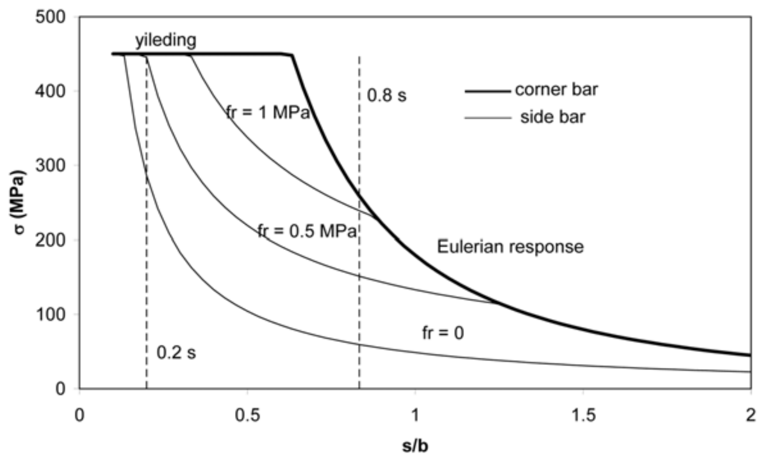

Fig. 7 Variation in critical stress with *s/b*

Analogously, with reference to the bar placed along the side of the transverse cross-section the stiffness of the system (see Fig. 6(b)) (in this case the stiffness represents the force necessary to produce a unit displacement along the direction perpendicular to the leg of the stirrups) at first yielding of the transverse steel is

$$\alpha_{eq} = \frac{192}{b_c^3} \cdot \left(E_{sec} \cdot \frac{s \cdot \delta^3}{12} + E_s \cdot \frac{\pi \cdot \omega_{st}^4}{64}\right) \tag{22}$$

Eq. (22) was derived assuming the cover and the stirrups to be beams loaded in flexure.

Finally, with reference to the case of the main bars in Fig. 6(c) the stiffness of the system proves to be expressed by

$$\alpha_{eq} = \frac{192}{b_c^3} \cdot \left(E_{sec} \cdot \frac{s \cdot \delta^3}{12} + E_s \cdot \frac{\pi \cdot \omega_{st}^4}{64}\right) + \frac{2 \cdot E_s \cdot \omega_{st}}{b_c} \tag{23}$$

By using the continuum approach, diffused springs can be assumed by introducing a fictitious parameter $k = \alpha_{eq}/s$ representing the stiffness per unit length. In this connection, a problem of an elastic beam on elastic springs subjected to an axial compressive load allows one to determine the critical load P_{crit} and the length L involved in the buckling phenomena of the longitudinal bars.

The Eulerian critical load of the longitudinal bars, considered as fixed between two stirrups, proves to be $P_E = \pi \cdot E \cdot I/s^2$, $I = \pi \cdot \phi_{long}^4/64$ being the inertia moment of the longitudinal bar.

To obtain the critical load, the energy method (see Russo and Terenzani 2001) was adopted, basing the choice of the shape on the buckled curve. The curve must satisfy the end bar condition $y(0) = y(L) = y'(L) = y'(0) = 0$.

Any shape of the deflection curve can be represented by a trigonometric series having the form

$$y(x) = \sum_{n=1}^{\infty} \frac{\delta_n}{2} \cdot \left[1 - \cos\left(\frac{2 \cdot \pi \cdot n}{L} \cdot x\right)\right] \tag{24}$$

which satisfies the boundary conditions and unilateral constrains due to the presence of a concrete core having higher stiffness than the concrete cover. The function $y(x)$ is the deflection ordinate and δ_n is the unknown amplitude value of anti-sinusoidal mode. By imposing an energy balance ensuring that the work done by the applied force P be equal to the increase in the total strain energy due to the energy of hoop deformation and of cover deformation plus the strain energy of bending of the buckled bar, it is possible to determine the critical load function of the critical length L and therefore the critical length as a lower bound of the function of the critical load.

Therefore the following expressions hold for the critical length L and the critical load P_{crit}

$$L = 2 \cdot \pi \cdot \left(\frac{E_r \cdot I}{3 \cdot k}\right)^{1/4} = 4.77 \cdot \left(\frac{E_r \cdot I}{k}\right)^{1/4} \text{ (in mm)} \tag{25}$$

$$P_{crit} = \sqrt{12 \cdot E_r \cdot I \cdot k} \quad \text{in N} \tag{26}$$

E_r being the reduced modulus proposed by Papia *et al.* (1988) and I the moment of inertia of the longitudinal bars.

By determining the length L the choice of the stress-strain curve in compression for longitudinal bars is made. The expressions obtained (see Eqs. (21), ..(29)) highlight the fact that the main parameters governing the overall instability of the main bars in the presence of FRC are the following: - diameter of stirrups and longitudinal bars; - stirrup spacing; - steel elasticity modulus; - elasticity secant modulus of SFRC (including, in accordance with the proposed model. the aspect ratio of fibers, the volume percentage of fibers, etc.); - side of the transverse cross-section; - and cover thickness. If we refer to the case of a member with square cross-section with main bars having 12 mm diameter and stirrups having 8 mm diameter, adopting Eq. (29) by means of Eq. (26) we obtain the variation in the critical stress with the variation in s/L shown in Fig. 7. The critical stress is here defined as the minimum value between f_y, P_{cr}/A_{li} and P_e/A_{li} ($i = 1$, 2 respectively for corner or side bar). Cases of plain and fibrous concrete with $f_r = 0$, 0.5 and 1.0 MPa are considered. From the graphs it clearly emerges that if the pitch of the stirrups is reduced (e.g., is lower than 0.5 b) the critical stress is f_y, while for the bars placed along the flat portion of the section its value is lower. As the fiber percentage increases the critical stress also increases, showing the efficiency in reducing the buckling effects of the main bars.

6. Stress-strain curves for transverse and longitudinal bars

To describe the compressive behavior of reinforced compressed members, the constitutive laws of longitudinal and transverse steel also need to be defined.

6.1 Stress-strain curves for steel in tension

For transverse steel with strain hardening behavior a three-linear-strain hardening model is assumed, as suggested in Dhakal and Maekawa (2002), in the following form

$$\sigma_s = \begin{cases} \varepsilon_s \cdot E_s & \text{for} \quad \varepsilon_s \le \varepsilon_y \\ f_y & \text{for} \quad \varepsilon_y \le \varepsilon_s \le 8 \cdot \varepsilon_y \\ \varepsilon_s \cdot E_s + (\varepsilon_s - \varepsilon_y) \cdot E_p & \text{for} \quad 8 \cdot \varepsilon_y \le \varepsilon_s \le 40 \cdot \varepsilon_y \end{cases} \tag{27}$$

E_p being the hardening modulus of the bilinear law and assumed to be equal to $0.03E_s$.

6.2 Stress-strain curves for steel in compression

The constitutive law assumed for a compressed longitudinal bar is given by Eq. (27), neglecting buckling effects. If buckling effects are considered, the average steel bar compressive stress-strain curve as written in Dhakal and Maekawa (2002) is here assumed in the form

$$\frac{\sigma}{\sigma_1} = 1 - \left(1 - \frac{\sigma^*}{\sigma_1^*}\right) \cdot \left(\frac{\varepsilon - \varepsilon_y}{\varepsilon^* - \varepsilon_y}\right) \quad \text{for} \quad \varepsilon_y < \varepsilon \leq \varepsilon^*$$

$$\sigma \geq 0.2 \cdot f_y; \quad \sigma = \sigma^* - 0.02 \cdot E_s \cdot (\varepsilon - \varepsilon^*) \quad \text{for} \quad \varepsilon > \varepsilon^* \tag{28}$$

with

$$\frac{\varepsilon^*}{\varepsilon_y} = 55 - 2.3 \cdot \sqrt{\frac{f_y}{100}} \cdot \frac{L}{\phi_1}; \quad \frac{\varepsilon^*}{\varepsilon_y} \geq 7$$

$$\frac{\sigma^*}{\sigma_1^*} = \alpha \cdot \left(1.2 - 0.016 \cdot \sqrt{\frac{f_y}{100}} \cdot \frac{L}{\phi_1}\right); \quad \frac{\sigma}{f_y} \geq 0.2 \tag{29}$$

α being 1 for linear hardening bars and 0.75 for perfectly elastic-plastic bars, and L being the buckling length.

Therefore the average monotonic stress-strain curve given by Eq. (29) shown in Fig. 5 can be assumed. In the same graph the graphical representation of Eq. (27) is also given. Both curves are dimensionless with respect to the yielding stress and to the corresponding strain.

Eq. (29) was derived by Dhakal and Maekawa (2002) as a result of microanalysis of bars with hardening behavior and it can be fully described in terms of the product of the square root of the yield strength and the slenderness ratio of the reinforcing bar, the latter being the ratio between the length L and the diameter of the longitudinal bar.

7. Load-carrying capacity and load-axial strain curves in compression

7.1 Load carrying capacity

The load-carrying capacity of reinforced concrete (R.C.) columns is determined as the sum of the three different strength contributions constituted by: - P_{cover} due to concrete cover area in a biaxial state of stresses; - P_{core} due to the concrete core area in a triaxial stress state of stresses; - and P_{sl} due to the longitudinal bars including buckling phenomena.

By considering the concrete contributions one obtains

$$P_u = \zeta \cdot f_c \cdot 4 \cdot \delta \cdot (b - \delta) + f_{cc} \cdot (b - 2 \cdot \delta)^2 \tag{30}$$

The contribution due to longitudinal bars is

$$P_s = A_{l1} \cdot \sigma_{s1} + \mathrm{A}_{l2} \cdot \sigma_{s2} \tag{31}$$

σ_{s1} and σ_{s2} being the minimum values between f_y and the critical stress σ_{cr} (see Eq. (2) assuming $\sigma_{cr} = P_{cr}/A_1$).

If we denote with P_0 the load-carrying capacity of a gross section of concrete defined as

$$P_o = f_c \cdot b^2 \tag{32}$$

the ratio between P_u and P_0 proves to be

$$\frac{P_u}{P_o} = \frac{\zeta \cdot f_c \cdot 4 \cdot \delta \cdot (b-\delta) + f_{cc} \cdot (b-2\delta)^2}{f_c \cdot b^2} = 4 \cdot \xi \cdot \left(\frac{\delta}{b}\right) + \frac{f_{cc}}{f_c} \cdot \left(1 - 4 \cdot \frac{\delta}{b}\right) \tag{33}$$

while the ratio between the confined area of concrete and the gross area is

$$\frac{A_n}{A_g} = \frac{b^2 - 4 \cdot \delta \cdot (b-\delta)}{b^2} = 1 - \frac{4 \cdot \delta \cdot (b-\delta)}{b^2} \cong 1 - \frac{4 \cdot \delta}{b} \tag{34}$$

Comparing Eq. (34) and Eq. (33) it emerges that in the presence of confinement effect and concrete FRC cover the reduction in the bearing capacity is lower than the reduction in the gross area (see Eq. (34)).

By imposing the condition that the strength reduction due to cover spalling be balanced by the increase in strength due to the confinement effect it is possible to derive the minimum amount of transverse steel in the form.

$$\frac{P_u}{P_o} = 4 \cdot \xi \cdot \left(\frac{\delta}{b}\right) + \frac{f_{cc}}{f_c} \cdot \left(1 - 4 \cdot \frac{\delta}{b}\right) \geq 1 \tag{35}$$

Therefore from Eq. (35) by solving with respect to f_{cc}/f_c one obtains

$$\frac{f_{cc}}{f_c} \geq \frac{\left(1 - 4 \cdot \frac{\delta}{b}\right)}{4 \cdot \xi \cdot \frac{\delta}{b}} \tag{36}$$

Considering Eqs. (10), (12) and Eq. (14) one obtains

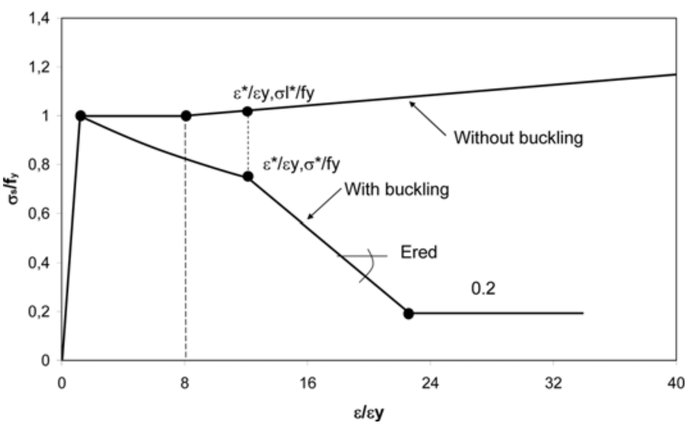

Fig. 8 Stress-strain relationships in compression for steel bars

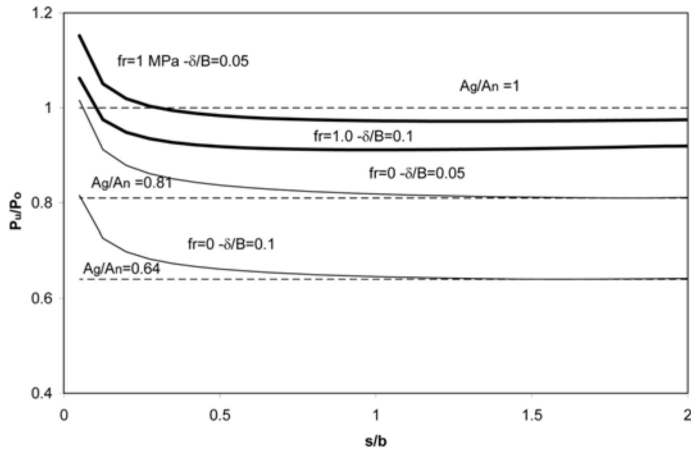

Fig. 9 Variation in load-carrying capacity with *s /b*

$$\frac{f_{cc}}{f_c} \cong 1 + \frac{2.1}{f_c^{0.7}} \cdot \left\{ \left[\left(\frac{2 \cdot \omega_{st1}}{(b-2\cdot\delta)\cdot s} + \frac{\sqrt{2}\cdot\omega_{st2}}{(b-2\cdot\delta)\cdot s} \right) \cdot f_y + \frac{2\cdot\delta}{b-2\cdot\delta} \cdot f_r \right] \cdot k_e \right\}^{0.7} \tag{37}$$

Substituting Eq. (37) in Eq. (36) gives

$$1 + \frac{2.1}{f_c^{0.7}} \cdot \left\{ \left[\left(\frac{2 \cdot \omega_{st1}}{(b-2\cdot\delta)\cdot s} + \frac{\sqrt{2}\cdot\omega_{st2}}{(b-2\cdot\delta)\cdot s} \right) \cdot f_y + \frac{2\cdot\delta}{b-2\cdot\delta} \cdot f_r \right] \cdot k_e \right\}^{0.7} \geq \frac{1-4\cdot\frac{\delta}{b}}{4\cdot\xi_{\mathrm{FRC}}\cdot\frac{\delta}{b}} \tag{38}$$

Eq. (38) allows one to obtain the minimum pitch of transverse steel to verify Eq. (35).

Fig. 9 gives the variation in the load-carrying capacity (Eq. (33)) with the variation in *s/b* for fixed values of post-cracking tensile strength of FRC and *δ/b* ratio. The cases examined refer to configuration a) in Fig. 2 and to stirrups having diameter 8 mm and 450 MPa yielding stress. The concrete had strength 40 MPa and side b of 400 mm. The comparison clearly shows that by adding fibers (also when a high cover value is adopted) the reduction in strength due to cover spalling is reduced.

7.2 Load-axial strain curves in compression

To determine the complete axial load-axial strain curve it will be assumed that the full load P is the sum of the three different strength contributions defined before.

Specifically, the procedure is based on the following steps: - an initial value of axial shortening ε is assumed; - the lateral strain $\varepsilon_t = \nu \cdot \varepsilon$ is computed assuming a fixed variation law of ν with ε (Eq. (9)); - the effective confinement pressure due to the transverse steel is computed; - the compressive strength of the confined concrete and corresponding strain is calculated using Eqs. (10), (17); the strength contribution due to the concrete cover is calculated through Eq. (1) by taking Eq. (17) into account; and finally σ is determined by means of Eq. (1). Repeating this procedure for all possible axial strain values the complete load-strain curve is plotted.

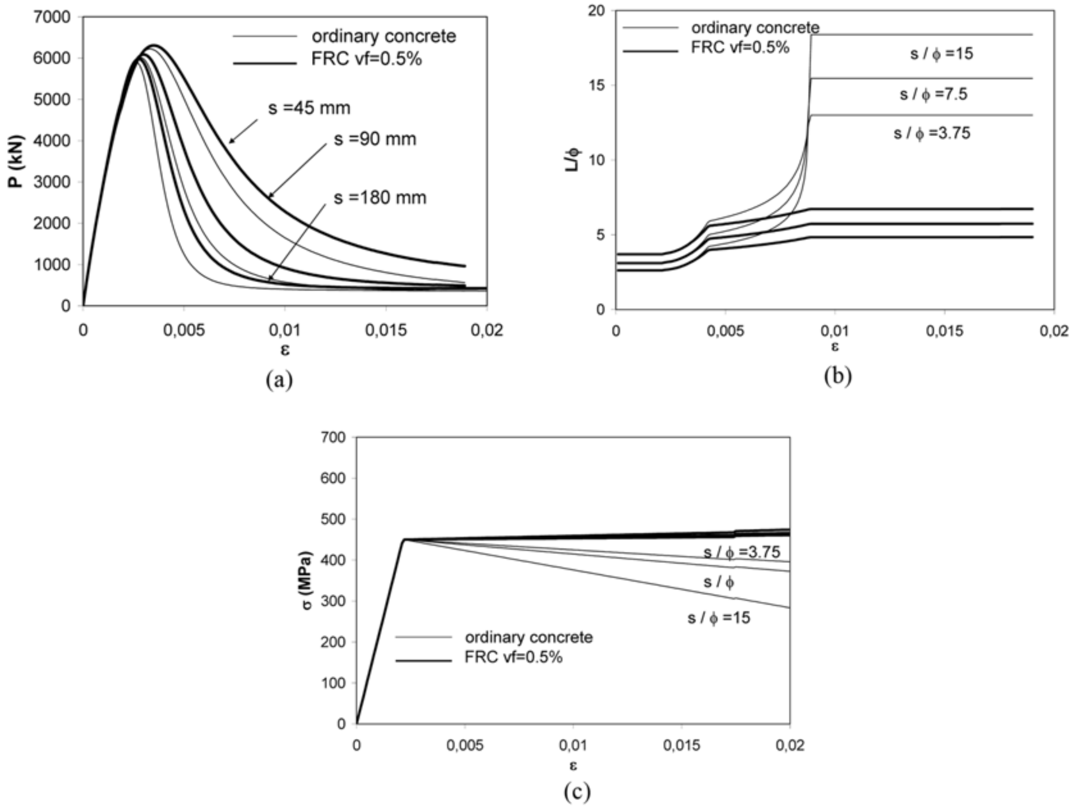

Fig. 10 Responses of a short plain concrete and a short fibrous HSC column (a) load-axial strain curves, (b) L/ϕ variation with axial strain, (c) stress in main steel with variation in axial strain

To explain the procedure, Fig. 10(a, b, c) shows the compressive response of a short column with square cross-section having external side b = 300 mm, reinforced with 8 longitudinal deformed bars having diameter ϕ = 12 mm and transverse stirrups having 8 mm diameter at pitch s = 45, 90, 180 mm. A cover δ = 20 mm is considered. The yield stress of longitudinal and transverse steel was assumed to be 450 MPa, while the cylinder compressive strength of the plain concrete specimen was 80 MPa. Hooked steel fibers having aspect ratio 60 and volume percentage 0.5% were considered.

Fig. 10(a) gives the load-axial strain curves for the three different pitches of stirrups for ordinary and fibrous concrete columns respectively for normal and high strength compressed members. Fig. 10(b) gives the corresponding variation in the critical length with respect to the diameter of longitudinal bars with the variation in axial strain; Fig. 10(c) gives the stress-strain curves adopted for steel bars in compression.

From the graphs it emerges clearly that the addition of fibers produces significant improvement in the performance of the columns, especially referring to the stability condition of longitudinal bars. Moreover, when fibers are used the strength contribution due to the yielding of the main bars is also present after the peak load is reached for the different pitches examined, including cases of slender bars. This aspect can be explained by the fact that in the case of FRC the presence of significant values of post-peak tensile strength of the composite ensures that the critical length L is reduced and its value is enclosed in the pitch *s* (or in a lower value) of the stirrups.

8. Comparison of analytical and experimental results

In this section a comparison is made between the analytical results generated here and the experimental ones given in the literature. Experimental data provided by Ganesan and Murthy (1990), Campione *et al*. (2007) and Zaina and Foster (2005) are used.

The first data refer to the experimental research carried out by Ganesan and Murthy (1990) and specifically to compressive tests on normal strength fiber reinforced concrete columns having a square cross-section, in the presence of longitudinal and transverse steel. The cases examined refer to prismatic members having 1000 mm length and square transverse cross-section with external side 200 mm and an effective cover of 25 mm. The columns were reinforced with 8 deformed bars having a 12 mm diameter and with transverse stirrups having 6 mm diameter placed at pitches of 60, 90, 180 and 240 mm. The yield stress of the transverse and longitudinal bars was 468 MPa. The concrete had a cylinder compressive strength of 20 MPa (measured on a 150×300 mm cylinder). Hooked steel fibers having aspect ratio 70 and volume percentage 1% were added to fresh concrete.

The second case examined refers to experimental research carried out by Campione *et al*. (2007) and specifically to compressive tests on normal strength fiber reinforced concrete columns having a square cross-section, in the presence of longitudinal and transverse steel. The cases examined refer to prismatic members having length 1200 mm and square transverse cross-section with side 210 mm and effective covers of 10 and 25 mm respectively. The columns were reinforced with 4 deformed bars having a 12 mm diameter and with stirrups having a 6 mm diameter placed at a pitch of 65 mm. The yield stress of the longitudinal and transverse bars was 461 MPa. The concrete had a cylinder compressive strength of 29 MPa (measured on a 100×200 mm cylinder) with corresponding strain of 0.0019. Hooked steel fibers having aspect ratio 55 and volume percentage 1% were added to fresh concrete, giving maximum compressive strength up to 32 MPa and corresponding strain of 0.0023.

The third case examined refers to experimental research carried out by Zaina and Foster (2005) and specifically to compressive tests on high strength fiber reinforced concrete columns having a square cross-section, in the presence of longitudinal and transverse steel. The columns were cast using high strength concrete with and without fibers. Different arrangements of transverse steel were also considered. The columns, having a side of 200 mm and overall length 2100 mm, were reinforced with 8 deformed bars having a 12 or 16 mm diameter and with closed transverse stirrups having a 6 mm diameter placed at a pitch of 50, 72, 100 and 150 mm, respectively. The cover was assumed to be equal to 20 mm. The yield stress of the longitudinal and transverse bars was 500 MPa. The fibrous concrete had a cylindrical compressive strength of 101 MPa for series R with a fiber content of 50 kg/m^3, 87 MPa for series Z and M with fiber contents of 50 and 65 kg/m^3 respectively. Details of specimens are presented in Table 1. Hooked steel fibers having aspect ratio 84 were added to fresh concrete.

Fig. 11(a) and Fig. 11(b) show the stress-strain curves of confined core (ordinary and fibrous concrete) experimentally determined by Ganesan and Murthy (1990) and ones determined analytically, showing good agreement.

Table 1 Geometrical and mechanical characteristics of confined specimens

Ref.	Specimen designation	V_f	ρ_s	Ultimate load (kN)		Ultimate strain	
				Experiment.	Predicted	Experiment.	Predicted
Ganesan and Murthy (1990)	R1	0	0.006	902.24	909	0.0027	0.0024
	R2	0	0.008	931.67	921	0.0029	0.0027
	R3	0	0.016	1029.74	1010	0.0032	0.0035
	R4	0	0.024	1118.00	1095	0.0034	0.0045
	F1	1.5	0.006	1000.31	1095	0.0032	0.0044
	F2	1.5	0.008	1059.16	1113	0.0043	0.0059
	F3	1.5	0.016	1157.23	1172	0.0052	0.0065
	F4	1.5	0.024	1260.20	1222	0.0073	0.0068
Campione *et al*. (2007)	A1	0	0.0054	1286	1173	0.0025	0.0027
	A2	1	0.0054	1398	1254	0.0032	0.0030
Zaina and Foster (2005)	4HF0-50R6r	0.65	0.0075	3438	3575	0.0041	0.0034
	4HF0-100R6r	0.65	0.0039	3326	3476	/	0.0031
	2HF0-150Z6r	0.65	0.0026	2962	2714	0.0027	0.0023
	2HF0-72M6r	0.85	0.0054	2586	2773	/	0.0033
	2HF0-100M6r	0.85	0.0039	3061	3092	/	0.0031
Average and standard deviation				Exp/Predicted = 1.0045		Exp/Predicted = 0.969	
				ST.DEV. = 0.058		ST.DEV. = 0.17	

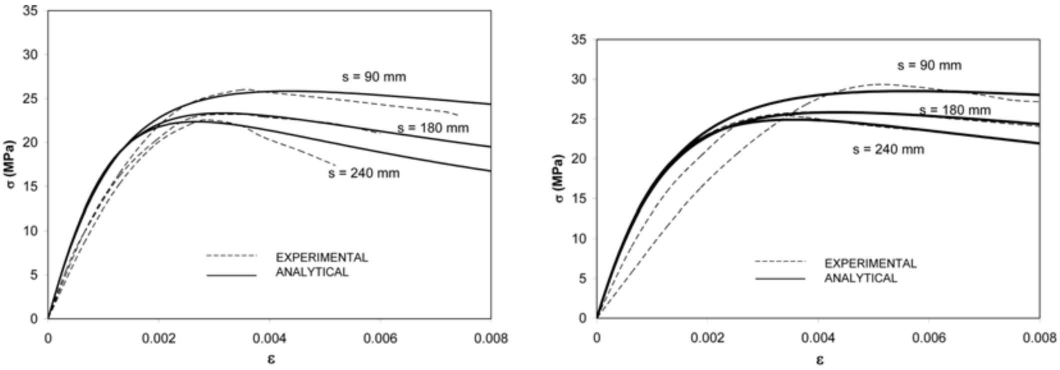

(a) $V_f = 0.00$ (b) $V_f = 1.00$ %

Fig. 11 Experimental and analytical stress-strain curve for confined FRC with hooked steel fibers: data of Genesa and Murthy (1990)

Finally, Fig. 12 shows a comparison between the analytical and experimental responses of columns tested in Campione *et al*. (2007). In both cases good agreement is observed both in the ascending and in the descending branches. Table 1 gives the experimental ultimate load and the corresponding strain (if available) for the different cases examined. In the same table the values predicted with the proposed model and the average and standard deviation values are also given.

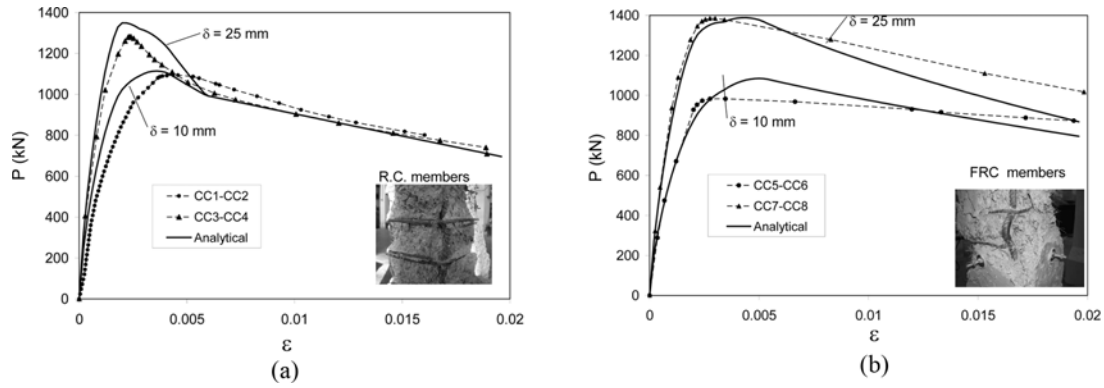

Fig. 12 Comparison between analytical and experimental load-axial strain curves: date of Campione *et al.* (2007)

9. Conclusions

In the present paper an analytical model is presented that is able to analyze the compressive behavior of short compressed fiber reinforced concrete columns with square cross-sections and different arrangements of longitudinal and transverse steel bars.

The model considers the effects of fibers on the overall stability of compressed longitudinal bars, on the interaction between concrete cover and confinement pressures and on the effectively confined concrete core at rupture.

The paper highlights the influence of the most relevant confinement parameters, i.e., type, volumetric ratio, spacing, yield strength, concrete grade, geometrical properties of fibers (length, diameter) and fiber volume, dimension of the transverse cross-section and cover thickness, highlighting some advantages and disadvantages in using fibers for structural members. The main results obtained are: - the calibration of stress-strain curves in compression for several grades of concrete, both plain and FRC; - the derivation of the softening coefficient for the biaxial state of stresses in FRC concrete cover; - the derivation of a simplified expression for prediction of the load-carrying capacity; - the derivation of the minimum amount of transverse steel able to ensure that the strength reduction due to the cover spalling is balanced by the strength increase of confined core.

The model was verified against data obtained from concentric compressive tests on concrete specimens reinforced with transverse steel and fibers.

References

ACI Committee 318 (2005), "Building code requirements for reinforced concrete (ACI 318-95), and Commentary ACI 318RM-02", *American Concrete Institute*, Detroit, Michigan.

Adepegba, D. and Regan, P. (1981), "Performance of steel fibre reinforced concrete in axially loaded short columns", *Int. J. Cement Light-W. Concrete*, **3**(4), 255-259.

Ahmad, S.H. and Shah, S.P. (1985), "Behaviour of hoop confined concrete under high strain rates", *ACI Mater. J.,* **82**(5), 634-647.

Aoude, H., Cook, W.D. and Michell, D. (2009), "Behavior of columns constructed with fibers and selfconsolidating concrete", *ACI Struct. J.*, **106**(3), 349-357.

Barros, J.A.O. and Figureiras, J.A. (1999), "Flexural behaviour of SFRC: testing and modeling", *J. Mater. Civil Eng.-ASCE*, **11**(4), 331-339.

Bencardino, F., Rizzuti, L. and Spadea, G. (2008), "Stress-strain behavior of steel fiber-reinforced concrete in compression", *J. Mater. Civil Eng.-ASCE*, **20**(3), 255-263.

Bentur, A. and Mindess, S. (1990), *Fibre Reinforced Cementitious Composites*, Elsevier Applied Science, Publishers Ltd., New York.

Campione, G., Mindess, S. and Zingone, G. (1999), "Compressive stress-strain behavior of normal and high strength carbon-fibre concrete reinforced with steel spirals", *ACI Mater. J.*, **91**(1), 27-34.

Campione, G. and La Mendola, L. (2001), "Stress-strain behavior in compression of steel - fibre lightweight concrete under monotonic and cyclic loads", *Proceedings of the Third Conference on Earthquake Resistant Engineering Structures*, Malaga, Spain, September.

Campione, G. (2002), "The effects of fibres on the confinement models for concrete columns", *Can. J. Civil Eng.*, **29**, 742-750.

Campione, G., La Mendola, L. and Papia, M. (2006), "Ultimate shear strength of fibrous reinforced concrete beams with stirrup", *Struct. Eng. Mech.,* **24**(1), 107-136.

Campione, G., Fossetti, M., Papia, M. and Priolo, S. (2006), "Experimental analysis of flexural behavior of fibrous reinforced concrete columns", *Proceedings of the CTE Conference*, Parma, Italy, September. (in Italian)

Campione, G. (2008), "Simplified flexural response of fibrous concrete beams", *J. Mater. Civil Eng.-ASCE*, **20**(4), 283-293.

Campione, G., Cucchiara, C., Mangiavillano, M.L. and Miraglia, N. (2009), "Flexural response of ordinary and fibrous reinforced concrete deep beams", *Atti del 13º Convegno Nazionale L'Ingegneria Sismica in Italia*, Bologna, Giugno-Luglio. (in Italian)

Cusson, D. and Paultre, P. (1994), "High-strength concrete columns confined by rectangular ties", *J. Struct. Eng.-ASCE,* **120**(3), 783-804.

Cusson, D. and Paultre, P. (1995), "Stress-strain model for confined high-strength concrete", *J. Struct. Eng.-ASCE,* **121**(3), 468-477.

Demeke, A. and Tegos, I.A. (1994), "Steel fiber reinforced concrete in biaxial stress tension-compression conditions", *ACI Struct. J.*, **91**(5), 579-584.

Dhakal, R.P. and Maekawa, K. (2002), "Reinforcement stability and fracture of cover concrete in RC members", *J. Struct. Eng.-ASCE*, **128**(10), 1253-1262.

Dhakal, R.P. (2006), "Post-peak response analysis of SFRC columns including spalling and buckling", *Struct. Eng. Mech.*, **22**(3), 311-330.

Dhakal, R.P. and Maekawa, K. (2002), "Modeling for post-yield buckling of reinforcement", *J. Struct. Eng.-ASCE*, **128**(9), 1139-1147.

Elwi, A.A. and Murray, D.W. (1979), "A 3D hypoelastic concrete constitutive relationship", *J. Eng. Mech.-ASCE*, **105**, 623-641.

Ezeldin, A.S. and Balaguru, P.N. (1992), "Normal and high strength fibre reinforced concrete under compression", *J. Mater. Civil Eng.-ASCE*, **4**(4), 415-427.

Fanella, D.A. and Naaman, A.E. (1985), "Stress-strain properties of fibre reinforced mortar in compression", A*CI J., Proceedings* No. 82-41, 475-483.

Foster, S.J. (2001), "On behavior of high-strength concrete columns, cover spalling, steel fibres, and ductility", *ACI Struct. J.,* **98**(4), 583-589.

Foster, S.J. and Attard, M.M. (2001), "Strength and ductility of fibre-reinforced high-strength concrete columns", *J. Struct. Eng.-ASCE*, **127**(1), 28-34.

Genesan, N. and Murthy, J.V.R. (1990), "Strength and behavior of confined steel fibre reinforced concrete columns", *ACI Mater. J.,* **87**(3), 221-227.

Hsu, L.S. and Hsu, C.T. (1994), "Stress-strain behaviour of steel-fiber-high strength concrete under compression", *ACI Struct. J.*, **91**(4), 448-457.

Lim, T.Y., Parasivam, P. and Lee, S.L. (1987), "An analytical model for tensile behaviour of steel fibre concrete", *ACI Mater. J.*, **84**(4), 286-298.

Mander, J.B., Priestley, M.J.N. and Park, R. (1988), "Theoretical stress-strain model for confined concrete", *J. Struct. Eng.-ASCE*, **114**(8), 1804-1826.

Mansur, M.A., Ong, K.C.G. and Parasivam, P. (1986), "Shear strength of fibrous concrete beams without stirrups", *J. Struct. Eng.-ASCE,* **112**(9), 2066-2079.

Nataraja, M.C., Dhang, N. and Gupta, A.P. (1999), "Stress-strain curves for steel-fibre reinforced concrete under compression", *Cement Concrete Compos.*, **21**, 383-390.

Naaman, A.E. (2003), "Strain hardening and deflection hardening fibre reinforced cement composites", *Proceedings of the IV International RILEM Workshop on High Performance Fibre Reinforced Cement Composites (HPFRCC4)*, Ann Arbour, MI, US.

Papia, M., Russo, G. and Zingone, G. (1988), "Instability of longitudinal bars in RC columns", *J. Struct. Eng.-ASCE,* **114**(2), 445-461.

Quintero-Febres, C.G., Parra-Montesionos, G. and Wight, J.K. (2006), "Strength of struts in deep concrete members designed using strut-and-tie method", *ACI Struct. J.*, **103**(4), 577-586.

Razvi, R. and Saatcioglu, M. (1999), "Confinement model for high-strength concrete", *J. Struct. Eng.-ASCE*, **125**(3), 281-289.

Russo, G. and Terenzani, L. (2001), "Non linear buckling model for the longitudinal reinforcement in RC columns", Studies and Research Graduate school in concrete structures - Fratelli Pesenti, Politecnico di Milano, Italy, Vol. 22, 303-227.

Sargin, M. (1971), "Stress-strain relationship for concrete and the analysis od structural concrete sections", Study No. 4, Solid Mechanics Division, University of Waterloo.

Saeker, P.K. (2001), "Fibre reinforced high strength concrete columns", *Proceedings of the International Conference on Adding Value Through Innovation*, Concrete Inst. of Australia, Perth, September.

Soroushian, P. and Lee, C.D. (1989), "Constitutive modelling of steel fibre reinforced concrete under direct tension and compression", Fibre Reinforced Cements and Concrete (Eds. Swamy, R.N and Barr, B.), Recent Developments, 363-375.

Zaina, M. and Foster, S.J. (2005), "Testing of concentric and eccentrically loaded fibre-reinforced HSC columns", UNICIV REPORT NoR-437, The University of New South Wales Sydney 2052 Australia ISBN:85841 4040 X.

Notations

A_{sl1} : area of longitudinal steel bars at the corners
A_{sl2} : area of longitudinal steel bars at the flat portion
b : external width of square section
b_c : width of concrete core of square R.C. members
E_s : modulus of elasticity of steel
E_r : reduced modulus of elasticity of longitudinal steel
E_t : tangent initial modulus of elasticity of concrete in tension
E_f : modulus of elasticity of fiber
E_{ctf} : tangent initial modulus of elasticity of fibrous concrete in tension
F : reinforcing index
f_c : peak longitudinal compressive stress of stress-strain curves of unconfined concrete
f_{ctf} : peak stress of fibrous concrete in tension
f_{ctu} : post-cracking stress of fibrous concrete in tension
f_t' : peak stress of plain concrete in tension
f_{cc} : peak longitudinal compressive stress of stress-strain curves of confined concrete
f_l : lateral confining stress acting on concrete
f_{le} : effective lateral confining stress acting on concrete
f_{yl} : yield strength of longitudinal steel
f_y : yield strength of steel stirrups
fr : post-cracking tensile strength
L : length of buckled bar
L_f : equivalent length of fiber
I : moment of inertia of longitudinal steel bar
k_2 : confinement effectiveness coefficient
P_e : Eulerian load of longitudinal bar on the length s
P_{crir} : critical load of longitudinal bar in the length L
k : stiffness for unit length of stirrups and cover
ke : effectiveness coefficient
s : centre-to-centre spacing of spirals, hoops of stirrups
s' : interior spacing between sets of transverse steel reinforcement
s_1 : distance between two successive longitudinal bars
v_f : volume percentage of fibers
α : stiffness of single stirrups and cover
β : shape parameter of stress-strain curve
δ : effective cover of stirrup
ε_{ct} : peak tensile strain in concrete
ε_{ctf} : peak tensile strain in fibrous concrete
ε_{cc} : strain at peak stress of confined concrete
ε_o : strain at peak stress of unconfined concrete
ε_s : strain value of stirrups in tension
ε_y : yielding strain of stirrups in tension
ε_t : tensile strain in concrete
ε_u : ultimate strain of stirrups in tension
ϕ_{long} : diameter of longitudinal bar
ρ_{st} : ratio of volume of transverse reinforcement to volume of concrete core
ϖ_{st1} : area of external transverse cross-section of stirrup
ϖ_{st2} : area of internal transverse cross-section of stirrup